

Grounding Points Model for Safety Enhancement in Autotransformer Configuration Railway System

Manuel S. Alvarez-Alvarado^{1,2*}, Zafar A. Khan^{3,4}, Anzar Mahmood⁴, Angel A. Recalde², Fernando Vaca-Urbano² and Abdullah Altamimi⁵

1. Department of Electrical and Computer Engineering, New Jersey Institute of Technology, Newark, United States of America
2. Facultad de Ingeniería en Electricidad y Computación, Escuela Superior Politécnica del Litoral, Guayaquil, Ecuador
3. Department of Electronics, Electrical and Systems Engineering, University of Birmingham, Birmingham, United Kingdom
4. Electrical Power Engineering, Mirpur University of Science and Technology, Mirpur, Pakistan
5. Department of Electrical and Computer Engineering, Majmaah University, Majmaah, Saudi Arabia

* **Corresponding Author:** E-mail: manuel.alvarez.alvarado@ieee.org,

Abstract

Electrified Urban Massive Transportation Railway Systems require the supply of electric power that complies to electromagnetic and safety standards, as well as operational regulation. This paper presents a mathematical modelling of a complete Autotransformer Configuration Railway System. The innovation of this study relies on the consideration of grounding points to calculate realistic rail voltages to perform safety improvements. This research incorporates the Carson's Line model to accurately depict the self- and mutual- impedances between the conductors of the railway system. A case study is simulated using real-world rail data from a quad-track AT railway system located in United Kingdom. The results have proven that the inclusion of grounding points in the load model significantly reduces the rail voltage resulting from self- and mutual- induction, thus increasing the effectiveness and robustness in achieving more realistic voltage calculations and enhancing safety level for improved industry practices.

Keywords: AC railway system; autotransformer; Carson's Line; grounding points; mathematical model; power flow

1. Introduction

Nowadays, the use of Urban Massive Transportation Systems has become an integral part of human activity. Railway Transportation Systems can be either electrified or non-electrified. Although the non- electrified railway systems accounts for the majority of existent railways worldwide [1], the electrified railway systems are much relevant due to its high reliability and efficiency if compared to its non-electrified counterpart and even other transportation technologies. Most of the electrified rail networks in the world are in European countries. These rail networks must meet the BS EN 50163 [2] and IEC 60850 [3] voltage standards. Regarding the electromagnetic standards and safety levels as a major concern, they must follow EN 50121 [4]. As the use of electrified rail networks have been increasing in the last decades, the impact of electric current on humans is currently under extended research. Therefore, rigorous safety levels have been established and standards compel to follow permissible values for body currents to evade any related incidents, e.g. electrocution.

However, to meet safety standards, the IEEE Standard 80 [5] might help the grounding standard problem in railway traction systems. The accessible touch voltages are classified as long-term and short-term time duration events. A more detailed description is presented in Table 1.

The big challenge is to determine the maximum permitted potential on the rail and safeguard proper electrification, while meeting safety standards. Recent research [4–6] show the amount of efforts invested in developing efficient and improved control systems to design transportation facilities in the USA including DC and AC traction power systems. The EN 50121 [4] is used in the UK for railway specifications, fixed installations, electrical safety, and earthing and return circuits. These standards show the limits for safe touch and step potential, which is widely used in the transportation industry for traction power substation grounding. There are algorithms for railways power flow that obviate grounding points and Carson's line. If these parameters are ignored in the model, it causes great impact on determining accurate rail voltages. For this reason, this paper focuses on steady-state condition and it

proposes a comprehensive mathematical model that considers the effects of grounding points and Carson’s line leading to a more realistic rail voltage calculation.

Table 1: Maximum Permissible Effective Touch Voltages U_t in AC Traction Systems

t (seconds)	$U_{t,max}$ long-term (Volts)	$U_{t,max}$ short-term (Volts)
>300	60	-
300	65	-
1	75	-
0.9	80	-
0.8	85	-
0.7	90	-
<0.7	-	155
0.6	-	180
0.5	-	220
0.4	-	295
0.3	-	480
0.2	-	645
0.1	-	785
0.05	-	835
0.02	-	865

The rest of the paper is structured as follows. Section II presents an overview of electric railway systems, section III describes the electric railway traction line. In section IV, the Carson’s line theory to quantify the mutual and self-impedance of railway conductors is outlined. Section V continues with the mathematical model of all components in the railway system; section VI presents the sequential load flow method for power flow simulation, and in section the case study is proposed. The results of the case study are shown in section VIII and finally section IX brings to the conclusions.

2. Electric Railway Systems

Power systems for electric railways can be broadly classified in DC traction and AC traction systems. DC traction railways requires rectified DC power supply obtained from AC sources through Traction Substations (TS) [1], and its voltage selection depends on the expected power demand and the length of the railway’s lines. Typically, a 600 V – 750 V is used in tramways; while 1500 V is used for a metro system. Substations, known as Traction Substations (TS) are connected to the electric high-voltage side distribution system [9] and the DC power supply is obtained through rectifiers, as shown in Fig. 1. On the other hand, AC railways systems provides power to AC motors with rectification step. A typical AC railway system substation is directly connected to one phase of a three-phase high-voltage supply grid. The high-voltage side is connected to the utility’s three-phase bus bar,

where its low-voltage side is connected to a single-phase bus bar [10]. A typical schematic is shown in Fig. 2. AC railways receives AC power straight from the grid usually at a different sub-synchronous frequency [1]. Single-phase secondary AC substations are directly connected to three-phase main supply high-voltage grid, thus composing a three-phase to two-phase power transformation [11].

There are mainly three types of AC railway power distribution. In the direct feeding configuration (DFC) shown in Fig. 3(a), AC power is directly connected to wagons. Although is simple and cost effective, it presents compensation problems and large power losses. Indeed, this configuration has high rail-to-earth voltage induction [12], and the electromagnetic interference with communication systems is not tolerable [4]. The booster transformer configuration (BTC) shown in Fig. 3(b), reduces electromagnetic interference to approximately 0.025 screening factor at 50 Hz, with 1 mile spacing between booster transformers (BT). The screening factor is defined as the ratio of the induced voltage in a disturbed circuit with compensation to the induced voltage without compensation. The leakage inductance of BT with a return conductor increases the total feeding impedance by approximately 50% compared with the direct feeding. Thus, the distance between two adjacent feeder substations is reduced due to the voltage drop along the contact wire [13]. However, adding 50 kV autotransformers (AT) at every 8-15 km intervals can increase substation distance up to 50-100 km. This configuration corresponds to an autotransformer feeding configuration (ATC) shown in Fig. 3(c). The AT has two symmetrical windings with its middle tap connected to the rails to provide earth potential for balancing the voltage between the contact wire and the return conductor.

The electromagnetic interference in ATC is normally lower than in the BT system. However, the size and MVA rating of the AT are much larger and more expensive than the BT. In addition, its protection equipment is more complex, and it needs additional installation clearance space [12].

The two most common electrified power supply systems for high speed rail and commuter rail lines are: 1×25 kV system and 2×25 kV systems. Both systems receive power from high-voltage, 60 Hz (in the US), 3-phase utility circuits and both systems provide 25 kV, 60 Hz, 1-phase power to the overhead catenary system. 1×25 kV systems utilize traction power supply stations with standard power supply transformers which provide power at 25 kV to the overhead. Other voltages are

possible, for example the Sanyo Shinkansen built in Japan (1972), which uses a 2:1 substation transformer with 60 kV supply and 30 kV [15]. Another example is the AMTRAK NE Corridor New Have/Boston line. This line uses four supply stations, three switching stations, and 16

paralleling stations. The advantage of the 2×25 kV system over the 1×25 kV AT system is well documented especially for high-speed trains and based on these criteria this paper focus on AT configuration.

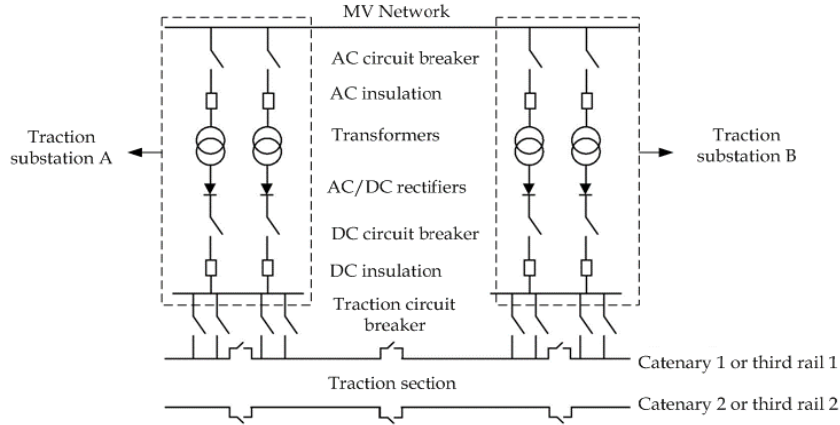


Fig. 1: Typical Traction Substation (TS) [14]

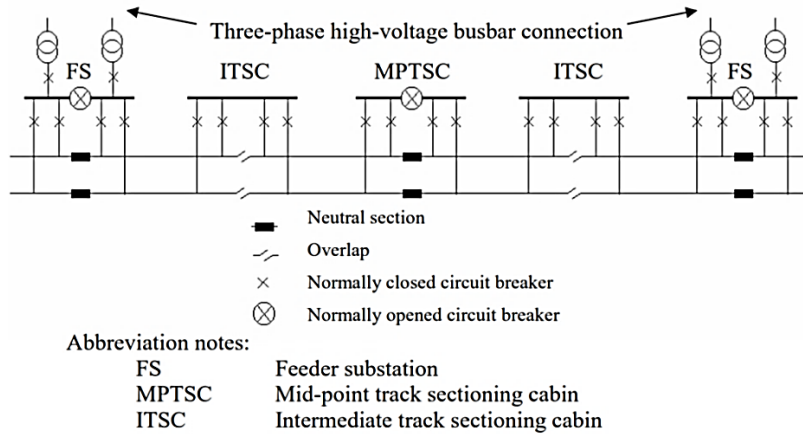


Fig. 2: Typical feeding diagram of a double-track 25 kV railway [12]

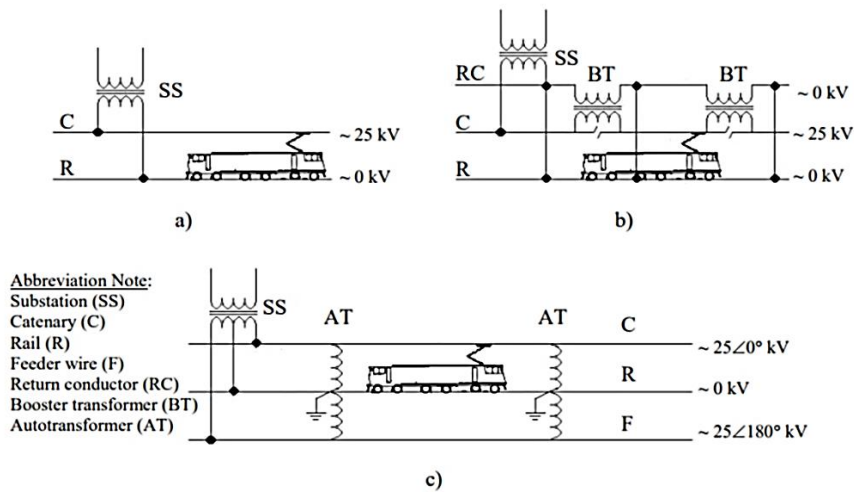


Fig. 3: Overhead catenary feeding systems for AC railways: (a) Direct feeding configuration; (b) Booster transformer feeding configuration; (c) Autotransformer feeding configuration [12]

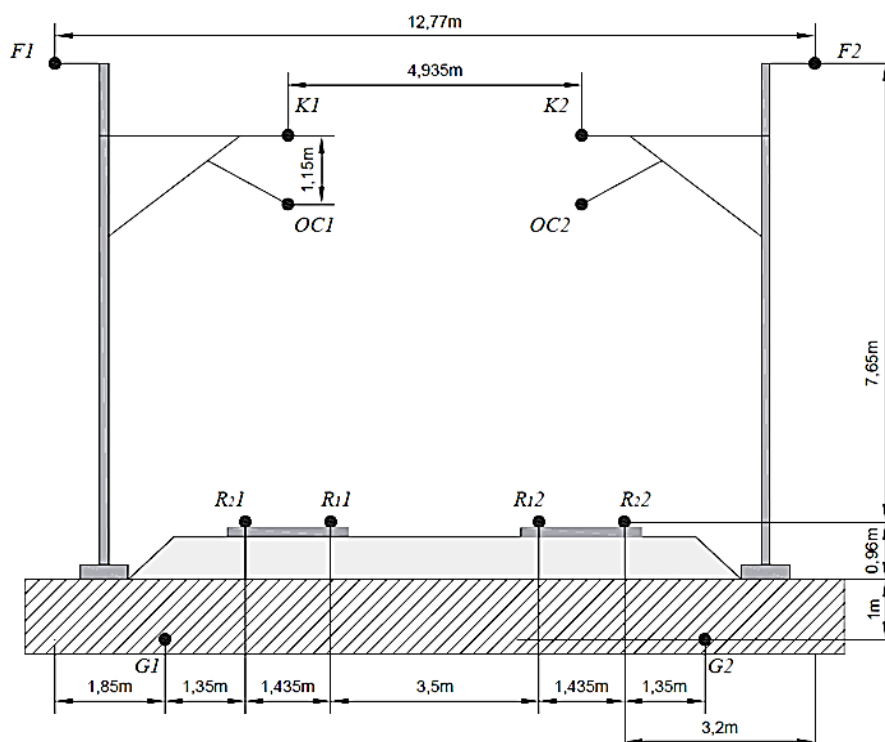


Fig. 4: Double-track based traction line right of way cross section [16]

3. Electric Railway Traction Line and Carson's Line

A typical cross section of a two tracks system is composed by 12 lines, which includes contact wires (OC1, OC2), messenger wires (K1, K2), feeders (F1, F2), rails (R1, R2), and ground wires (G1, G2), as shown in Fig. 4. In order to model the electric railway traction line, various simplifications were made. For instance, it is possible to combine different conductors into equivalent conductors:

- C: composed of K1, OC1, K2, and OC2.
- F: composed of F1 and F2.
- R: composed of R11, R12, R21, R22, G1 and G2.

An important consideration on the power flow is that there is a return current in the grounded neutral wires and earth. Hence, the mutual inductance cannot be neglected, and Carson's Theory should be applied.

If some conductors are grounded or the system is not balanced, earth will carry a return current [11]. Earth is considered to have a uniform resistivity, as well as semi-infinite characteristic. To consider the effect of earth currents on impedance calculations, Carson proposed the replacement of earth by a set of "earth return" conductors located directly under the overhead

conductors as shown in Fig. 5. The conductor aa^1 carries a current I_a with a return through circuit dd^1 beneath the surface of the earth. Carson's line can be thought as a single real conductor dd^1 with self-equivalent geometric mean distance equal to that of aa^1 located at a distance D_{ad} below the overhead line, where D_{ad} is adjusted so that the inductance calculated with this configuration is equal to the one measured by test.

The equations for the Carson's line are:

$$V_a - V_{a^1} = (z_{aa^1} - z_{ad^1})I_a \quad (1)$$

$$V_d - V_{d^1} = (z_{ad^1} - z_{dd^1})I_a \quad (2)$$

The given voltages are measured with respect to the same reference, V_d . By subtracting (2) from (1):

$$V_d - V_{d^1} - V_a + V_{a^1} = (z_{ad^1} - z_{dd^1} - z_{aa^1} + z_{ad^1})I_a \quad (3)$$

Since $V_d = 0$ and $V_{a^1} - V_{d^1} = 0$, then:

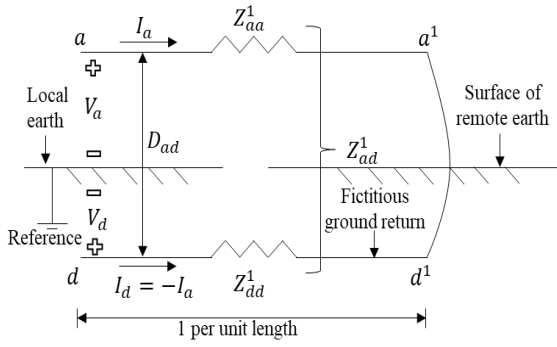
$$V_a = (z_{aa^1} + z_{dd^1} - 2z_{ad^1})I_a \quad (4)$$

However, the relation between the voltage and current in conductor "a" can be expressed in function of the self-impedance as:

$$V_a = z_{aa}I_a \quad (5)$$

Hence:

$$z_{aa} = z_{aa^1} + z_{dd^1} - 2z_{ad^1} \quad (6)$$


Fig. 5: Carson's line diagram

Considering an extra conductor called “ k ”, the mathematical expression that describes the mutual impedance between conductors is as follows:

$$z_{ak} = z_{ak^1} + z_{dd^1} - 2z_{ad^1} \quad (7)$$

The self-impedance per unit of length is defined as follows:

$$z_{aa^1} = r_a + 2\pi f \times 10^{-4} \ln\left(\frac{1}{GMR_a}\right) \quad (8)$$

where r_a is the resistance per unit length of conductor “ a ” (Ω/km), f is the frequency of the system (Hz), GMR_a is Geometric Mean Radius (ft).

Similarly,

$$z_{dd^1} = r_d + 2\pi f \times 10^{-4} \ln\left(\frac{1}{D_{ad}}\right) \quad (9)$$

The mutual impedance between conductor “ a ” and “ k ” without considering the ground effect, depends on the distance between conductors (D_{ak}) given in ft. The mathematical expression is defined as:

$$z_{ak^1} = 2\pi f \times 10^{-4} \ln\left(\frac{1}{D_{ak}}\right) \quad (10)$$

The mutual impedance per unit length between conductor “ a ” and its image reflected to ground is:

$$z_{ad^1} = 2\pi f \times 10^{-4} \ln\left(\frac{1}{D_{ad}}\right) \quad (11)$$

Replacing (8), (9) and (11) into (6) and regrouping factors, the self-impedance per km is given by:

$$z_{aa} = (r_a + r_d) + j 4\pi f \times 10^{-4} \ln\left(\frac{D_{ad}}{GMR_a}\right) \quad (12)$$

Replacing (8), (9) and (10) into (7) and regrouping factors, the mutual impedance per km is given by:

$$z_{ak} = r_d + j 4\pi f \times 10^{-4} \ln\left(\frac{D_{ad}}{D_{ak}}\right) \quad (13)$$

The resistance r_d is a value that depends on the frequency of the system given in Ω/km [13]:

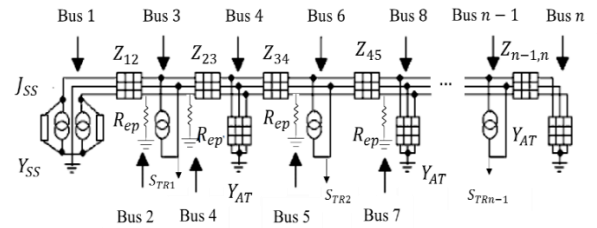
$$r_d = 9.87 \times 10^{-4} f \quad (14)$$

The term D_{ad} is the distance between conductor a and its image d given feet, which depends on the resistivity of the ground ρ and the frequency of the system f (Carson, 1926):

$$D_{ad} = 2160.43\sqrt{\rho/f} \quad (15)$$

4. AC Railway System Modelling

To perform simulation studies on a railway traction power system, all electrical components of the network must be modelled. A relationship between the voltages and the current at the terminals of the component must be found. These components include wires used for power transmission including the rails and earth wires, the autotransformers, the substation transformers, and the trains. By joining all the elements, the equivalent circuit of the system is presented in Fig. 6.


Fig. 6: AC railway equivalent circuit

4.1 Conductor Wires

Each bus of the AC Railway system has 12 separate conductors, which are grouped into three groups (C, R and F). The impedance matrix representing the CRF conductor set connected between two adjacent buses (i and j) is:

$$Z_{ij} = \begin{bmatrix} C & R & F \\ Z_{CC} & Z_{CR} & Z_{CF} \\ Z_{RC} & Z_{RR} & Z_{RF} \\ Z_{FC} & Z_{FR} & Z_{FF} \end{bmatrix} \begin{matrix} C \\ R \\ F \end{matrix} \quad (16)$$

4.2 Substation

Fig. 7 shows the equivalent circuit of the substation.

By defining $Z'_1 = \frac{Z_1}{(2a)^2}$; $Z_A = Z'_1 + Z_2$; $Z_B = Z_2 + 4Z_e$, the substation can be modelled using its admittance matrix Y_{SS} and injected current J_{SS} , which can be written as follows:

$$Y_{SS} = \begin{bmatrix} \frac{1}{Z_A} + \frac{1}{Z_B} & \frac{2}{Z_B} & \frac{1}{Z_A} - \frac{1}{Z_B} \\ \frac{2}{Z_B} & -\frac{4}{Z_B} & \frac{2}{Z_B} \\ \frac{1}{Z_A} - \frac{1}{Z_B} & \frac{2}{Z_B} & \frac{1}{Z_A} + \frac{1}{Z_B} \end{bmatrix} \begin{matrix} C \\ R \\ F \end{matrix} \quad (17)$$

$$J_{SS} = \frac{V'_0}{Z_A} \begin{bmatrix} 1 \\ 0 \\ -1 \end{bmatrix} \begin{matrix} C \\ R \\ F \end{matrix} \quad (18)$$

Hence, the mathematical model that represent the power substation is [12]:

$$\begin{bmatrix} J_C \\ J_R \\ J_F \end{bmatrix} = \frac{V'_0}{Z_A} \begin{bmatrix} 1 \\ 0 \\ -1 \end{bmatrix} + \begin{bmatrix} \frac{1}{Z_A} + \frac{1}{Z_B} & \frac{2}{Z_B} & \frac{1}{Z_A} - \frac{1}{Z_B} \\ \frac{2}{Z_B} & -\frac{4}{Z_B} & \frac{2}{Z_B} \\ \frac{1}{Z_A} - \frac{1}{Z_B} & \frac{2}{Z_B} & \frac{1}{Z_A} + \frac{1}{Z_B} \end{bmatrix} \begin{bmatrix} V_C \\ V_R \\ V_F \end{bmatrix} \quad (19)$$

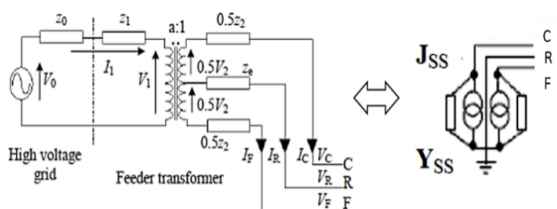


Fig. 7: Power substation model for the AT railway system [12]

4.3 Autotransformer

Models for all the components of an AT power network were proposed [17-18]. The autotransformer equivalent circuit is as shown in Fig. 8. The admittance matrix is given by:

$$Y_{AT} = \begin{bmatrix} \frac{1}{2Z_{gt}} - \frac{1}{Z_{mt} + 2Z_{gt}} & \frac{1}{2Z_{gt}} + \frac{1}{Z_{mt} + 2Z_{gt}} \\ -\frac{1}{Z_{gt}} & \frac{2}{Z_{gt}} \\ \frac{1}{2Z_{gt}} - \frac{1}{Z_{mt} + 2Z_{gt}} & -\frac{1}{Z_{gt}} + \frac{1}{Z_{mt} + 2Z_{gt}} \end{bmatrix} \begin{matrix} C \\ R \\ F \end{matrix} \quad (20)$$

Then, the mathematical model that describes the autotransformer is as follows:

$$\begin{bmatrix} J_C \\ J_R \\ J_F \end{bmatrix} = \begin{bmatrix} \frac{1}{2Z_{gt}} - \frac{1}{Z_{mt} + 2Z_{gt}} & \frac{1}{2Z_{gt}} + \frac{1}{Z_{mt} + 2Z_{gt}} \\ -\frac{1}{Z_{gt}} & \frac{2}{Z_{gt}} \\ \frac{1}{2Z_{gt}} - \frac{1}{Z_{mt} + 2Z_{gt}} & -\frac{1}{Z_{gt}} + \frac{1}{Z_{mt} + 2Z_{gt}} \end{bmatrix} \begin{bmatrix} V_C \\ V_R \\ V_F \end{bmatrix} \quad (21)$$

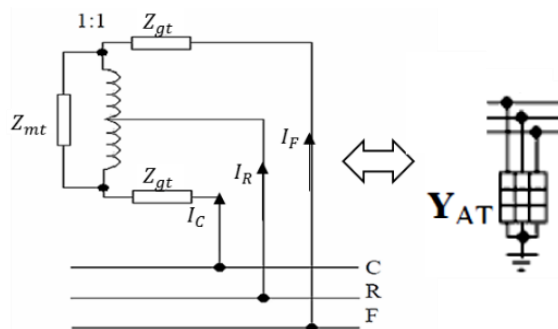


Fig. 8: Autotransformer equivalent circuit [8]

4.4 Electric Trains

The trains can be modelled as a current source, hence:

$$I_{TRi} = \left(\frac{S_{TRi}}{V_i^C - V_i^R} \right)^* \begin{bmatrix} 1 \\ -1 \\ 0 \end{bmatrix} \begin{matrix} C \\ R \\ F \end{matrix} \quad (22)$$

Notice that i corresponds to the bus number where the train is placed and the symbol “*” represents the conjugate value of the mathematical expression.

4.5 Grounding points

This is modelled as a resistance connected between rail and ground. The value and location of grounding points can vary depending on the system. In this paper, the value of this equivalent resistance is considered to be 25 Ω and they are located every half mile [5]. Those values are obtained based on private communication with industry professionals. The mathematical model of the grounding point is as follows:

$$I_{epi} = \left(\frac{V_i^R}{R_{ep}} \right) \begin{bmatrix} 0 \\ 1 \\ 0 \end{bmatrix} \begin{matrix} C \\ R \\ F \end{matrix} \quad (23)$$

5. AC Railway Power Flow

There are many different methods to run a power flow. In this paper the Sequential Load Flow Method (SLFM) is employed due to its simplicity and effectiveness in comparison with other methods. The analysis starts by defining the voltage at bus i (V_i) and current circulating from

bus i to j (I_{ij}) are complex vectors consisting of three components (C, R, F) as given:

$$V_i^T = [|V_i^{(C)}| \angle \delta_i^{(C)} \quad |V_i^{(F)}| \angle \delta_i^{(F)} \quad |V_i^{(R)}| \angle \delta_i^{(R)}] \quad (24)$$

$$I_{ij}^T = [|I_{ij}^{(C)}| \angle \alpha_{ij}^{(C)} \quad |I_{ij}^{(F)}| \angle \alpha_{ij}^{(F)} \quad |I_{ij}^{(R)}| \angle \alpha_{ij}^{(R)}] \quad (25)$$

Consider an AC railway power system with n buses as the one shown in Fig. 6. By applying Kirchhoff's current law, the current-balance equation of bus i can be obtained by:

$$\begin{bmatrix} Y_{11} & Y_{12} & \dots & Y_{1n} \\ Y_{21} & Y_{22} & \dots & Y_{2n} \\ \vdots & \vdots & \ddots & \vdots \\ Y_{n1} & Y_{n2} & \dots & Y_{nn} \end{bmatrix} \begin{bmatrix} V_1^Y \\ V_2^Y \\ \vdots \\ V_n^Y \end{bmatrix} = \begin{bmatrix} J_1^Y \\ J_2^Y \\ \vdots \\ J_n^Y \end{bmatrix}; \gamma = C, R, F \quad (26)$$

In a compact form, can be rewritten as:

$$[Y]_{3n \times 3n} [V]_{3n \times 1} = [J]_{3n \times 1} \quad (27)$$

The matrix $[Y]_{3n \times 3n}$ is known as the bus admittance matrix, which can be constructed from the admittance of the substation, line and autotransformer. The elements Y_{ij} are formed as follows [19]:

$$Y_{ii} = \text{sum of admittances connected to bus } i; \quad (28)$$

$$Y_{ij} = -\text{sum of admittances connected to bus } i \text{ and } j \quad (29)$$

On the other hand, the current J_i^Y is the injected current into conductor γ of node i . If in node i a train is located, then the injected current is equal to the current drawn by the train ($J_{TR,i}$). Then, mathematically:

$$J_i^Y = -J_{TR,i} \begin{bmatrix} 1 \\ -1 \\ 0 \end{bmatrix} \begin{matrix} C \\ R \\ F \end{matrix} \quad (30)$$

For the substation, the injected current flows through the catenary and feeder. Thus, its expression is:

$$J_i^Y = J_{SS} \begin{bmatrix} 1 \\ 0 \\ -1 \end{bmatrix} \begin{matrix} C \\ R \\ F \end{matrix} \quad (31)$$

Once the injected currents and the bus admittance matrix are defined, the following steps can be applied to develop the SLFM:

- Step I: Specify a tolerance level ε , which is a small positive number.
- Step II: Initialize values for the unknown voltages and define this as $V(1)$.

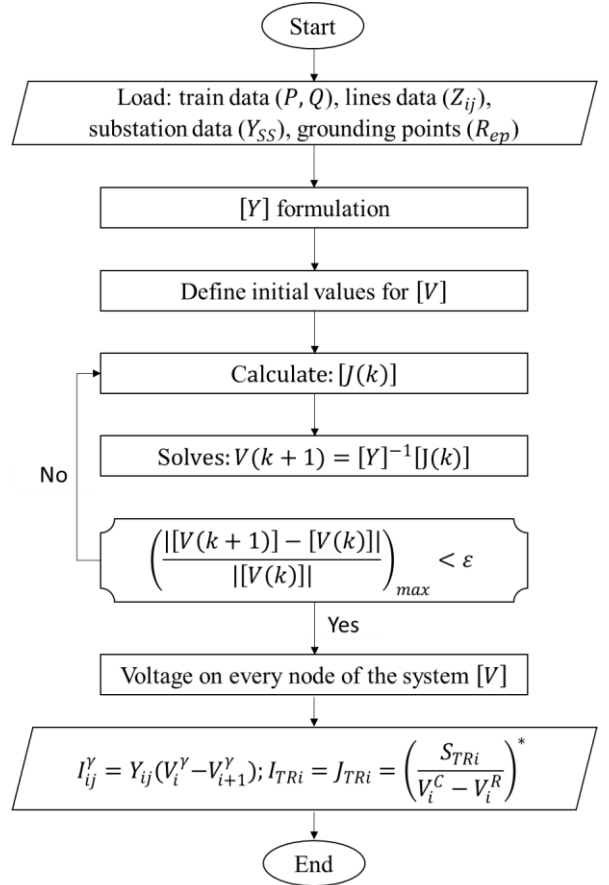


Fig. 9: Quad-track AT railway power feeding system

- Step III: Calculate $[J(k)]$, which is the injected current for iteration k in each node by using the defined voltages.
- Step IV: Calculate the updated bus voltage for the next iteration by applying:

$$V(k+1) = [Y]^{-1} [J(k)] \quad (32)$$

- Step V: Repeat step III to IV until the following condition is satisfied:

$$\left(\frac{|[V(k+1)] - [V(k)]|}{|[V(k)]|} \right)_{max} < \varepsilon \quad (33)$$

Once the voltages in each bus are known, the currents in each section of the line can be obtained by applying (35) and for the current train consumption (36).

$$I_{ij}^Y = Y_{ij}(V_i^Y - V_{i+1}^Y) \quad (34)$$

$$I_{TRi} = J_{TRi} = \left(\frac{S_{TRi}}{V_i^C - V_i^R} \right)^* \quad (35)$$

A general process of the methodology is presented in Fig. 9. The flowchart starts with the initialization of the inputs such as train, lines,

substation, and grounding points data. Then, the admittance matrix is formulated using (28) and (29). Next, the unknown voltages are initialized with values of 1.0 p.u. later, the current matrix is obtained using (30) and (31). This is followed by the determination of the voltages and this process is repeated until (33) is satisfied. Finally, the voltages on every node and the currents flowing through the lines of the system are obtained using (33)-(35).

6. Case Study

The system to analyse is a quad-track AT railway system with the properties given in Table 2 [12]. The number of trains per track is 4 and the complex power consumed by each train is $1.0 + j0.8$ p.u. on a 25 MVA base. The position (D) of each train is described in Table 3. In addition, an illustrative Quad-track AT railway system is presented in Fig. 10.

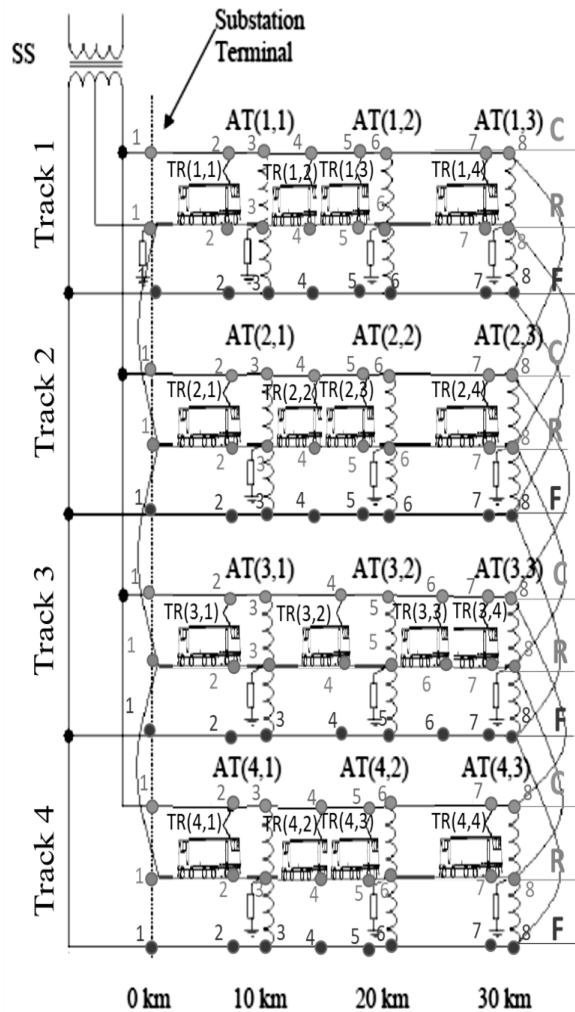


Fig. 10: Quad-track AT railway power feeding system

Table 2: AT Railway System Data

Substation:	25 MVA, 2x25 kV (AT feeding system) $Z_A = 3 + j27.22 \Omega$; $Z_B = 1 + j13.11 \Omega$
Autotransformer:	Leakage impedance = $0.1564 + j0.0997 \Omega$ Magnetizing impedance = $101.4 + j279.1 k\Omega$ Number of autotransformers per track = 3 Turn ratio = 1:1
Overhead catenary feeding system:	$Z_{OH} = \begin{bmatrix} 0.1192 + j0.7522 & 0.0574 + j0.3877 & 0.0568 + j0.3953 \\ 0.0574 + j0.3877 & 0.1648 + j0.6709 & 0.0571 + j0.3410 \\ 0.0568 + j0.3953 & 0.0571 + j0.3410 & 0.2036 + j0.8847 \end{bmatrix} \frac{\Omega}{km}$
Rail-to-earth ballast resistance =	10 Ω -km
Topology of the lines (Li, 2010):	<ul style="list-style-type: none"> • Average distance between center line of two tracks = 15 ft • Gauge = 4 ft 8-1/2 inch (standard gauge) • Contact wire height above rail level at supports = 17.5 ft • Messenger wire height above rail level at support = 22 ft • Both contact and messenger wires are assumed to be located vertically above the track center. • Negative feeder height above rail level = 23 ft • Negative feeder offset with respect to track center (towards outside) = 9 ft • Static (Aerial) ground wire height above rail level 20 ft • Static (Aerial) ground wire offset with respect to track center (towards outside) = 12 ft.
Resistivity for each conductor in [Ω /mi]:	$K1 = 0.2370$; $OC1 = 0.2323$; $F1 = 0.1601$; $K2 = 0.2370$; $OC2 = 0.2323$; $F2 = 0.1601$; $R_{11} = 0.0420$; $R_{21} = 0.0420$; $G1 = 0.6109$; $R_{12} = 0.0420$; $R_{22} = 0.0420$; $G2 = 0.6109$
GMR for each conductor in [ft]:	$K1 = 0.0186$; $OC1 = 0.0187$; $F1 = 0.0309$; $K2 = 0.0186$; $OC2 = 0.0187$; $F2 = 0.0309$; $R_{11} = 0.2660$; $R_{21} = 0.2660$; $G1 = 0.0105$; $R_{12} = 0.2660$; $R_{22} = 0.2660$; $G2 = 0.0105$

Table 3: Train Position

Track	Train number			
	1	2	3	4
	D (km)	D (km)	D (km)	D (km)
1	8.0	12.0	19.0	25.0
2	6.0	12.0	18.0	26.0
3	2.0	13.0	21.0	29.0
4	5.0	11.0	20.0	27.0

7. Results and Discussion

The self- and mutual- impedances between the wires are determined based on the topology of the system. The distances and impedances given in Table 2 in combination with Carson's line formulations given in Section 3, brings Table 4. The diagonal of Table 4 shows the self-impedances while the elements out of the diagonal are the mutual impedances. The results coincide with the ones given in [20].

Once the self- and mutual- impedances are obtained, a power flow can take place. A power flow program is developed in MATLAB, following the mathematical models described in previous sections.

Table 4: Self and mutual impedances of each conductor in Ω/mi

	K1	OC1	F1	K2	OC2	F2	R ₁	R ₂	G1	R ₂	R ₂	G2
K1	0.3323 + 1.4458i	0.0953 + 0.7800i	0.0953 + 0.6766i	0.0953 + 0.6339i	0.0953 + 0.6287i	0.0953 + 0.5738i	0.0953 + 0.6141i	0.0953 + 0.6141i	0.0953 + 0.6584i	0.0953 + 0.5897i	0.0953 + 0.5737i	0.0953 + 0.5621i
OC1	0.0953 + 0.7800i	0.3276 + 1.4452i	0.0953 + 0.6952i	0.0953 + 0.6287i	0.0953 + 0.6339i	0.0953 + 0.5768i	0.0953 + 0.5868i	0.0953 + 0.5868i	0.0953 + 0.6593i	0.0953 + 0.5701i	0.0953 + 0.5581i	0.0953 + 0.5623i
F1	0.0953 + 0.6766i	0.0953 + 0.6952i	0.2554 + 1.3843i	0.0953 + 0.5738i	0.0953 + 0.5768i	0.0953 + 0.5383i	0.0953 + 0.5688i	0.0953 + 0.5772i	0.0953 + 0.7871i	0.0953 + 0.5436i	0.0953 + 0.5312i	0.0953 + 0.5272i
K2	0.0953 + 0.6339i	0.0953 + 0.6287i	0.0953 + 0.5738i	0.3323 + 1.4458i	0.0953 + 0.7800i	0.0953 + 0.6766i	0.0953 + 0.5897i	0.0953 + 0.5737i	0.0953 + 0.5621i	0.0953 + 0.6141i	0.0953 + 0.6141i	0.0953 + 0.6584i
OC2	0.0953 + 0.6287i	0.0953 + 0.6339i	0.0953 + 0.5768i	0.0953 + 0.7800i	0.3276 + 1.4452i	0.0953 + 0.6952i	0.0953 + 0.5701i	0.0953 + 0.5581i	0.0953 + 0.5623i	0.0953 + 0.5868i	0.0953 + 0.5868i	0.0953 + 0.6593i
F2	0.0953 + 0.5738i	0.0953 + 0.5768i	0.0953 + 0.5383i	0.0953 + 0.6766i	0.0953 + 0.6952i	0.2554 + 1.3843i	0.0953 + 0.5436i	0.0953 + 0.5312i	0.0953 + 0.5273i	0.0953 + 0.5688i	0.0953 + 0.5772i	0.0953 + 0.7871i
R ₁	0.0953 + 0.6141i	0.0953 + 0.5868i	0.0953 + 0.5688i	0.0953 + 0.5897i	0.0953 + 0.5701i	0.0953 + 0.5436i	0.1373 + 1.1231i	0.0953 + 0.7745i	0.0953 + 0.5738i	0.0953 + 0.6796i	0.0953 + 0.6339i	0.0953 + 0.5430i
R ₂	0.0953 + 0.6141i	0.0953 + 0.5868i	0.0953 + 0.5772i	0.0953 + 0.5737i	0.0953 + 0.5581i	0.0953 + 0.5312i	0.0953 + 0.7745i	0.1373 + 1.1231i	0.0953 + 0.5863i	0.0953 + 0.6339i	0.0953 + 0.6008i	0.0953 + 0.5293i
G1	0.0953 + 0.6584i	0.0953 + 0.6593i	0.0953 + 0.7871i	0.0953 + 0.5621i	0.0953 + 0.5623i	0.0953 + 0.5273i	0.0953 + 0.5738i	0.0953 + 0.5863i	0.7062 + 1.5152i	0.0953 + 0.5430i	0.0953 + 0.5293i	0.0953 + 0.5180i
R ₁	0.0953 + 0.5897i	0.0953 + 0.5701i	0.0953 + 0.5436i	0.0953 + 0.6141i	0.0953 + 0.5868i	0.0953 + 0.5688i	0.0953 + 0.6796i	0.0953 + 0.6339i	0.0953 + 0.5430i	0.1373 + 1.1231i	0.0953 + 0.7745i	0.0953 + 0.5738i
R ₂	0.0953 + 0.5737i	0.0953 + 0.5581i	0.0953 + 0.5312i	0.0953 + 0.6141i	0.0953 + 0.5868i	0.0953 + 0.5772i	0.0953 + 0.6339i	0.0953 + 0.6008i	0.0953 + 0.5293i	0.0953 + 0.7745i	0.1373 + 1.1231i	0.0953 + 0.5863i
G2	0.0953 + 0.5621i	0.0953 + 0.5623i	0.0953 + 0.5273i	0.0953 + 0.6584i	0.0953 + 0.6593i	0.0953 + 0.7871i	0.0953 + 0.5430i	0.0953 + 0.5293i	0.0953 + 0.5180i	0.0953 + 0.5738i	0.0953 + 0.5863i	0.0953 + 1.5152i

Table 5: Voltage on quad-track AT railway system

Element	Results taken from [12]		Obtained results		Percentage difference	
	C (kV)	F (kV)	C (kV)	F (kV)	C (%)	F (%)
SS (1)	22.89	24.12	22.78	24.20	0.4835	0.2992
AT(1,1)	22.69	24.12	22.68	24.13	0.0471	0.0327
AT(2,1)	22.71	24.12	22.52	24.13	0.8265	0.0415
AT(3,1)	22.77	24.09	22.69	24.10	0.3587	0.0482
AT(4,1)	22.74	22.10	22.84	24.10	0.4758	9.0467
AT(1,2)	22.66	24.19	22.98	24.15	1.4012	0.1596
AT(2,2)	22.67	24.18	22.67	24.16	0.0229	0.0947
AT(3,2)	22.68	24.17	22.85	24.17	0.7388	0.0120
AT(4,2)	22.65	24.18	22.65	24.17	0.0044	4.1741
AT(1,3)	22.75	24.17	22.73	24.17	0.0976	0.0037
AT(2,3)	22.75	24.17	22.74	24.17	0.0343	0.0037
AT(3,3)	22.75	24.17	22.76	24.17	0.0369	4.1402
AT(4,3)	22.75	24.17	22.76	24.17	0.0369	0.0037
TR(1,1)	22.69	24.10	22.71	24.10	0.0630	0.0021
TR(2,1)	22.72	24.07	22.41	24.05	1.3821	0.0889
TR(3,1)	22.83	23.99	22.86	24.93	0.1217	0.2263
TR(4,1)	22.75	24.05	22.74	24.06	0.0659	0.0283
TR(1,2)	22.69	24.14	22.70	24.14	0.0150	0.0008
TR(2,2)	22.71	24.13	22.74	24.13	0.0022	0.0141
TR(3,2)	22.76	24.11	22.79	24.10	0.1199	0.0166
TR(4,2)	22.73	24.11	22.73	24.11	0.0141	0.0012
TR(1,3)	22.65	24.19	22.68	24.19	0.1466	0.0012
TR(2,3)	22.65	24.18	22.68	24.18	0.1298	0.0004
TR(3,3)	22.67	24.18	22.66	24.18	0.0309	0.0074
TR(4,3)	22.75	24.17	22.74	24.17	0.0189	0.0000
TR(1,4)	22.74	24.17	22.74	24.17	0.0018	0.0054
TR(2,4)	22.75	24.17	22.75	24.17	0.0044	0.0029
TR(3,4)	22.75	24.17	22.75	24.17	0.0022	0.0004
TR(4,4)	22.75	24.17	22.75	24.17	0.0013	0.0008

Nomenclature: TR(i,j) is train j on track i and AT(i,j) is autotransformer j on track i. SS represent the substation.

In order to show the efficacy of the proposed algorithm a power flow is run without considering the groundings points and then the results are compared with the one given in [12]. Table 5 reveals that feeder and catenary voltages are kept close to the nominal voltage, that is the system presents low voltage difference, leading to low power losses in the system. The obtained values in Table 5, present an error less than 2% in comparison with the ones given in [12], which brings high confidence to the proposed algorithm. The next results are the current consumed by each train. All the trains consume the same amount of current since they are consuming the same amount of power to operate. This fact is confirmed by the obtained results presented in Table 6.

On the other hand, to show the effect of the grounding points, Figs 11 and 12 are presented. In Fig. 11, the rail voltages are organized by train position and track. The Fig.11 is divided in two scenarios: a) no grounding points; b) considering grounding points. At first look, the presence of grounding points in the rail voltages is reduced, but not significantly. Nevertheless, a deeper analysis on it, reveals that rail voltages are reduced as the distance between analysed point and the train or autotransformer increases. This can be verified in Fig. 12, in which the rail voltages profile appears as a function of the distance. The Fig. 12 is divided in 4 sections and each of them represents one track of the system.

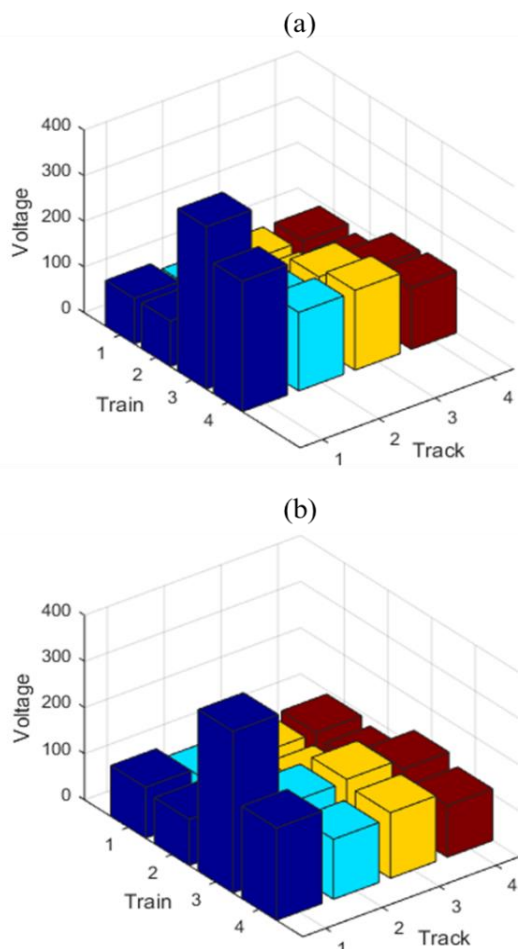


Fig. 11: Train Rail Voltage: (a) No grounding points; (b) Grounding points considered

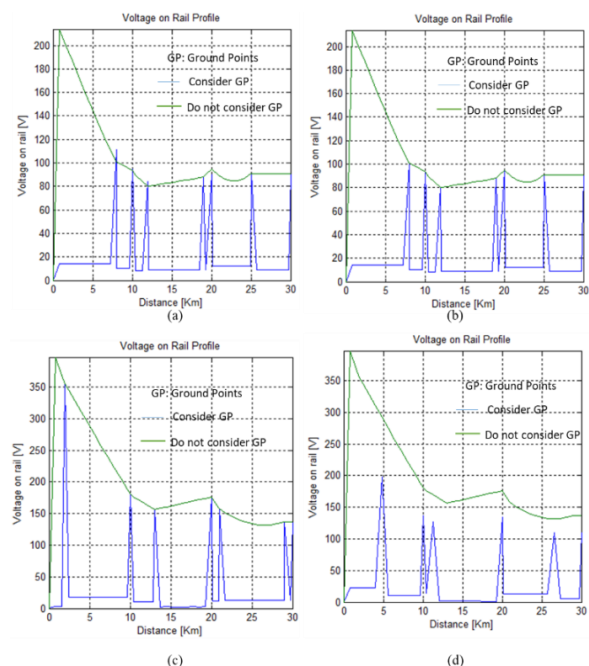


Fig. 12: Effect of grounding points on track: (a) 1; (b) 2; (c) 3; (d) 4

Table 6: Current consumed by each train

Train	Current [A]
TR(1,1)	51.52 \angle - 35.17°
TR(2,1)	50.87 \angle - 34.62°
TR(3,1)	50.13 \angle - 34.00°
TR(4,1)	51.79 \angle - 33.74°
TR(1,2)	51.97 \angle - 35.14°
TR(2,2)	51.55 \angle - 34.87°
TR(3,2)	51.33 \angle - 34.69°
TR(4,2)	52.64 \angle - 34.44°
TR(1,3)	52.51 \angle - 36.07°
TR(2,3)	53.36 \angle - 36.78°
TR(3,3)	53.21 \angle - 35.22°
TR(4,3)	53.47 \angle - 35.72°
TR(1,4)	52.08 \angle - 35.50°
TR(2,4)	51.57 \angle - 34.98°
TR(3,4)	51.37 \angle - 34.73°
TR(4,4)	50.98 \angle - 34.40°

8. Conclusion

A systematic modelling approach for autotransformer configuration of railway system power flow with the inclusion of grounding points is presented. Impact of grounding points on the load model is assessed. A case study using real-world rail data is simulated and the results suggest that introduction of grounding points significantly changes the voltage profile. The inclusion of grounding points in the power flow model lowers the rail voltage in comparison with the model without grounding points. The proposed approach provides a more realistic power flow model with enhanced accuracy by considering the grounding points and can potentially be extended to a dynamic power flow model. The key advantage of this approach includes the achievement of higher safety levels with lower rail voltages. Important future applications of the model proposed in this paper could include but not limit to short circuit analysis in railway power systems.

9. Acknowledgments

This study was supported by the Walter Valdano Raffo II program in Escuela Superior Politécnica del Litoral (ESPOL) and the Secretariat of Higher Education, Science, Technology and Innovation of the Republic of Ecuador (SENESCYT).

10. References

[1] Krastev, I., Tricoli, P., Hillmansen, S., & Chen, M. (2016). Future of Electric Railways: Advanced Electrification Systems with Static Converters for ac

- Railways. *IEEE Electrification Magazine*, 4(3), 6-14.
- [2] B. S. EN, “50163: 2004:“Railway applications,” *Supply voltages Tract. Syst.*
- [3] I. E. Commission, “Railway Applications—Supply Voltages of Traction Systems.” Standard IEC-60850, 2007.
- [4] Cozza, A., & DÉmoulin, B. (2008). On the Modeling of Electric Railway Lines for the Assessment of Infrastructure Impact in Radiated Emission Tests of Rolling Stock. *IEEE Trans. On Electromagnetic Compatibility*, vol. 50, no. 3, 566-576.
- [5] IEEE, *IEEE guide for safety in AC substation grounding*. IEEE, 2000.
- [6] Hu, S., Xie, B., Li, Y., Gao, X., Zhang, Z., & Luo, L. et al. (2017). A Power Factor-Oriented Railway Power Flow Controller for Power Quality Improvement in Electrical Railway Power System. *IEEE Transactions On Industrial Electronics*, 64(2), 1167-1177.
- [7] Hu, S., Li, S., Li, Y., Krause, O., Xie, B., & An, B. et al. (2018). A Balance Transformer-Integrated RPFC for Railway Power System PQ Improvement With Low-Design Capacity. *IEEE Transactions On Industrial Electronics*, 65(4), 2925-2934.
- [8] B. Mohamed, P. Arboleya, and M. Plakhova, “Current injection based Power Flow Algorithm for bilevel 2×25 kV railway systems,” in *Power and Energy Society General Meeting (PESGM), 2016*, 2016, pp. 1–5.
- [9] Bhim Singh, G. Bhuvaneswari & Vipin Garg. (2006). Improved Power Quality AC-DC Converter for Electric Multiple Units in Electric Traction. In *Power India Conference, 2006 IEEE* (p. 6–pp).
- [10] R. W. White, “AC supply systems and protection,” *Fourth Vocat. Sch. Electr. Tract. Syst. IEE Power Div.*, 1997.
- [11] I. M. ABDULAZIZ. (2003). *Mathematical Modelling and Computer Simulations of Induced Voltage Calculations in AC Electric Traction* (Doctor of Philosophy). Napier University, Edinburgh.
- [12] T. KULWORAWANICHPONG (2003). *Optimising AC electric railway power flows with power electronic control* (Doctor of Philosophy). The University of Birmingham.
- [13] Feng, J., Chu, W., Zhang, Z., & Zhu, Z. (2017). Power Electronic Transformer-Based Railway Traction Systems: Challenges and Opportunities. *IEEE Journal Of Emerging And Selected Topics In Power Electronics*, 5(3), 1237-1253.
- [14] M. A. Ríos, & G. Ramos. (2012). Power system modelling for urban massive transportation systems. In *Infrastructure Design, Signalling and Security in Railway* (pp. 179-202). InTech.
- [15] Hill, R. (1994). Electric railway traction. Part 3: Traction power supplies. *Power Engineering Journal*, 8(6), 275-286.
- [16] Kilter, J., Sarnet, T., & Kangro, T. (2014). Modelling of high-speed electrical railway system for transmission network voltage quality analysis: Rail Baltic case study. In *Electric Power Quality and Supply Reliability Conference (PQ)* (pp. 323-328). IEEE.
- [17] Z. Shao. (1988). *Auto-transformer power supply system for electric railways*. The University of Birmingham.
- [18] W. S. Chan. (1988). *Whole system simulator for AC traction*. The University of Birmingham.
- [19] J. D. Glover, M. S. Sarma, & T. Overbye. (2012). *Power System Analysis & Design, SI Version*. Cengage Learning.
- [20] Li, S. (2010). *Power flow in railway electrification power system*. New Jersey Institute of Technology, Department of Electrical and Computer Engineering.